Dolomite cation order in the geological record

Carlos M. Pina[1,2,*], Carlos Pimentel[1,2,#] and Ángel Crespo[1]

[1]*Departamento de Mineralogía, Petrología, Cristalografía y Geoquímica. Facultad de Ciencias Geológicas. Universidad Complutense de Madrid. c/ José Antonio Novais, 12. E-28040 Madrid, Spain.*

[2]*Instituto de Geociencias IGEO (UCM – CSIC). c/ Severo Ochoa, 7. E-28040 Madrid, Spain.*

ABSTRACT

Dolomite is a carbonate mineral frequently found in sedimentary rocks from Proterozoic to Holocene. In the Iberian Peninsula, dolomites appear in a wide number of geological formations and they can be considered as representative of dolomites crystallised in most (post)sedimentary environments on Earth. In this paper, we present a first systematic study of the cation order of dolomites formed from Neoproterozoic to late Holocene. We found that the lowest values of cation order (quantified by measuring $I_{01.5}/I_{11.0}$ intensity ratios on diffractograms) mainly correspond to dolomites formed in about the last 30 Myr. In contrast, older dolomites usually reach maximum $I_{01.5}/I_{11.0}$ intensity ratios. Furthermore, higher values of cation order seem to be related to higher values of the full width half maximum of 10.4 diffraction peaks ($FWHM_{10.4}$). Assuming that a decrease in $FWHM_{10.4}$ (i.e. an increase in the crystallite size) in sedimentary environments indicates mineral ripening, our results show that Mg-Ca ordering in dolomites might take place mainly by a dissolution-(re)crystallisation ageing process operating over large geological periods.

KEYWORDS

Dolomite, Iberian Peninsula, geological record, cation ordering, crystallite size, dissolution-crystallisation, X-ray Powder Diffraction.

[*]Corresponding author: cmpina@geo.ucm.es

[#] Current address: Departamento de Sistemas y Recursos Naturales, E.T.S.I. de Montes, Forestal y del Medio Natural, Universidad Politécnica de Madrid. C/ José Antonio Novais, 10. 28040 Madrid (Spain).

1. INTRODUCTION

The mineral dolomite [$CaMg(CO_3)_2$] was discovered by the geologist and mineralogist Déodat Gratet de Dolomieu during a journey through Northern Italy (de Dolomieu, 1791). Since Dolomieu's discovery, geologists have found that dolomite is a ubiquitous carbonate mineral, which mainly forms from seawater. However, despite its abundance in sedimentary rocks, and after more than two centuries of investigations, knowledge is still scant about the mechanism (or mechanisms) of dolomite formation. In the scientific literature, this lack of knowledge has been termed the *dolomite problem*, which can be expressed as follows: at present, large quantities of dolomite do not seem to form in nature under the geochemical conditions of the past sedimentary cycles.

In order to solve the *dolomite problem*, scientists have followed two main strategies: (i) performing crystallisation experiments using conditions similar to those inferred by geochemical data (Deelman, 2011 and references therein; Pimentel and Pina, 2014, 2016 and references therein; Gregg et al., 2015) and (ii) investigating the petrological, mineralogical and geochemical characteristics of natural dolomites in relation to their past and present formation conditions (e.g., Burns et al., 2000; Warren, 2000; Gregg et al., 2015).

The second research strategy has provided interesting data on relevant issues such as chemical and isotope composition of natural dolomites and natural water from which they formed, Mg/Ca ratios, and saturation states of seawater with respect to dolomite during the Phanerozoic, etc. (Burns et al., 2000; Riding and Liang, 2005; Li et al., 2015; Lu et al., 2018). In addition to these studies, estimates of dolomite abundance with respect to total carbonate in the geological record clearly indicate that dolomite was an important rock-forming mineral in the geological past, but it is relatively scarce in rocks formed in Cenozoic and Holocene times (Figure 1).

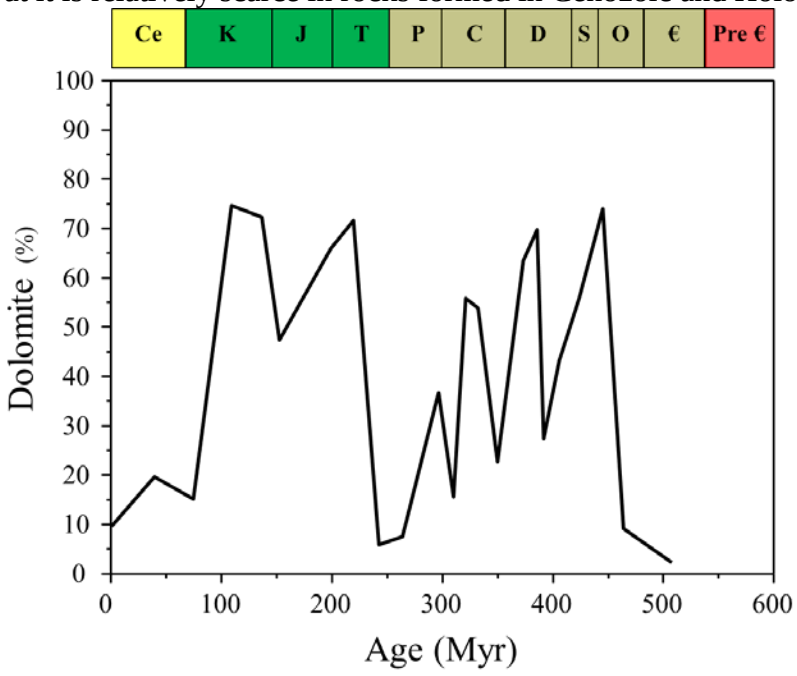

Figure 1. Abundance of dolomite with respect to total carbonate rock in the geological record (modified after Given and Wilkinson, 1987). Colour code: Cenozoic (yellow); Mesozoic (green); Palaeozoic (olive green); Precambrian (red).

Despite all of the valuable data currently available, crystallochemical information on natural dolomites and geochemical data of their formation environments is still incomplete. In particular, there is a lack of information on the variability of both the degree of Mg-Ca order and crystallite size (i.e. the size of the diffraction coherent domain) of dolomite crystals formed during geological time and under different petrogenic conditions. Yet, this information may be relevant to determine the mechanisms and kinetics of the chemical reactions that lead to the formation of extensive masses of dolostones. Since previous experimental works demonstrated that direct inorganic precipitation of fully-ordered dolomite is not possible at ambient conditions (Warren, 2000; Deelman, 2011), the study of the progressive ordering of Ca and Mg in carbonate rocks and sediments is crucial to understand the (re)crystallisation process that results in the formation of dolomite. In 1977, Gaines proposed the terms protodolomite and pseudodolomite to describe Mg-Ca carbonates with low degree of cation order and high magnesium calcites near to dolomite-stoichiometry without cation order, respectively. Although both terms are controversial and not universally accepted (Gregg et al., 2015, and references therein), they refer to magnesium calcium carbonates, which can potentially evolve to dolomites with high Mg-Ca order. In this regard, the time scale in which such a cation ordering occurs is still an open question.

In this paper, we present new data on the cationic order of dolomites found in the Iberian Peninsula and formed in the last 775 Myr, i.e., from late Neoproterozoic to late Holocene. Taking into account both the variety of their rock formation environments and the key position of the Iberian Plate during the continent evolution of the Earth, Iberian dolomites can be considered as representative of most sedimentary dolomites formed on our planet.

The findings reported in this paper provide new insights into the possible mechanisms and time scales in which the cationic ordering of natural dolomites may occur.

2. MATERIALS AND METHODS

2.1. Dolomite sampling

More than 100 hand samples of dolomites were collected in 34 localities, geolocalised and labelled to be subsequently studied. Prior to this field work, geological maps of Spain at scale 1:50000 (MAGNA series) and literature on regional and local geology were reviewed in order to locate dolomite outcrops of different ages and geological environments. These environments include fluvial lacustrine systems in continental basins, shallow and medium to deep marine basins, and, more scarcely, caves with active speleothem formation. The age of sampled dolomites ranged from late Precambrian to late Holocene, including Palaeozoic, Mesozoic and Cenozoic dolomite formations. The age of each dolomite formation was taken from the information contained in the dossiers on the MAGNA maps, published by the Spanish Geological Survey.

2.2. X-ray powder diffraction

Small fragments of collected samples were ground and sieved to a particle size <53 μm to be studied with X-ray powder diffraction (XRPD). Diffraction was performed with a Siemens D-500 diffractometer equipped with a CuKα source (λ = 1.54 Å). Recorded diffractograms were subsequently analysed with XPowder software (Martin, 2008) and dolomite was identified in the samples using the PDF2 database (PDF numbers 75-1710 and 84-1208). The Mg-Ca order of dolomites was quantified by calculating $I_{01.5}/I_{11.0}$ intensity ratios (McKenzie, 1981; Pimentel and Pina, 2014 and references therein). In addition, the full width half maximum of 10.4 diffraction peaks ($FWHM_{10.4}$) was measured.

2.3. Optical microscopy

Thin sections of a selected number of dolomite samples were examined with an optical microscope (Nikon Eclipse Ci POL) equipped with a camera Nikon D5500. Microphotographs were taken at a magnification of 50X, 100X and 200X, and under plane and cross-polarised light. Standard thin sections of dolomite samples were prepared in the laboratory of Mineralogy and Petrology at the Complutense University of Madrid. First, rock samples were cut and mounted on standard 2.8 cm × 4.8 cm glass slides. Then, the thickness of the dolomite sections was reduced by polishing with a Rotpol-35 (Struers) to a standard value of 30 µm.

2.4. Scanning electron microscopy and Energy Dispersive X-ray Spectrometry (SEM-EDX)

Thin sections of dolomite samples were also imaged by scanning electron microscopy (SEM, JEOL JSM 6400-40 kV) and chemically analysed with a Link-analytical EDX system. For this purpose, thin sections were coated with gold or carbon. Compared to carbon coating, the use of gold allowed us to record SEM images of optimal quality and resolution.

3. RESULTS

Dolomites studied in this work were collected from various rock formations corresponding to ancient geological environments that contributed to the construction of the Iberian Peninsula (Figures 2 and 3, Table 1; polar coordinates of all sampling locations are provided in Supplementary Information Table ST-1).

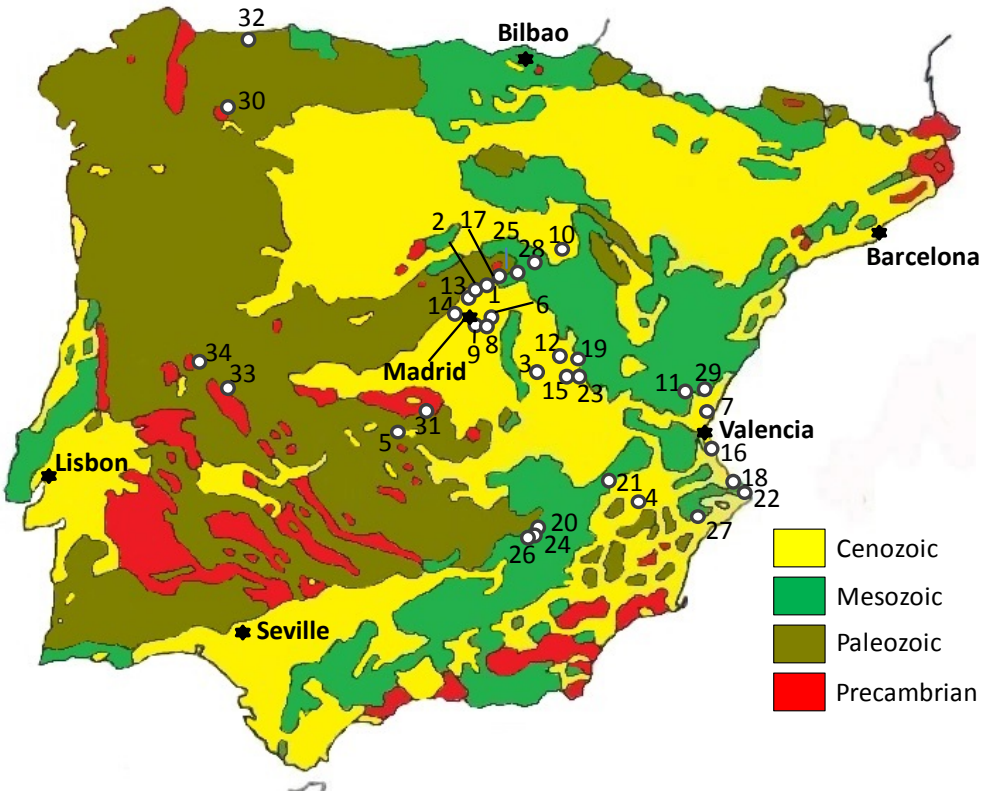

Figure 2. Simplified geological map of the Iberian Peninsula showing dolomite sampling locations (see Table 1). Polar coordinates of all sampling locations are given in Supplementary Information Table ST-1.

Figure 3. Examples of outcrops where dolomite samples were collected. (a) Cambrian marine dolostone (El Emperador, Toledo, Spain); (b)Triassic marine dolostone (indicated by a white arrow) (Torrechiva, Castellón, Spain); (c) Cave in Cretaceous marine massive dolostone (Sepúlveda, Segovia, Spain) and (d) Cenozoic dolostone from a continental basin (Ribesalbes, Castellón, Spain).

Reviewed geological information has shown that all the collected dolomites were formed at temperatures not far from ambient temperature. In our study, we have excluded dolostones presumably originated or affected by metamorphic and/or hydrothermal events, as well as clastic rocks formed by grains from previous dolostones (e.g., conglomerates or breccias). Inspection of thin sections of dolomite samples with the optical microscope allowed us to locate adequate areas for subsequent SEM imaging and EDX analysis. In addition, optical microscopy images provided a first glimpse of the shape and size of dolomite crystals and their textural relation with other minerals, i.e., calcite, quartz and gypsum. Even though a systematic analysis of thin sections was not performed, we observed that the size of dolomite crystals is usually larger in older dolostones than in most recent ones, indicating different degrees of (re)crystallisation (Figure 4). In most cases, dolomite crystals are euhedral or subeuhedral.

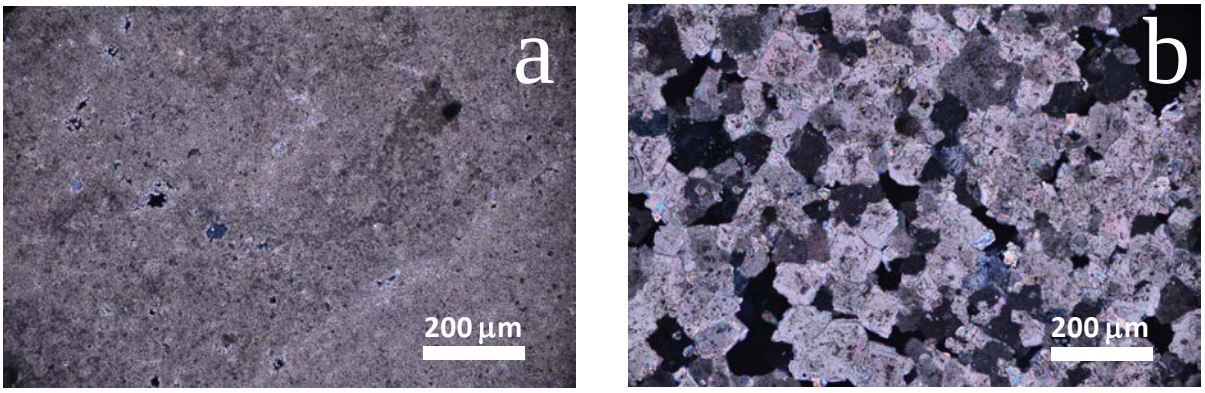

Figure 4. Optical microscope photographs taken under cross-polarised light of dolostone thin sections. (a) Cenozoic dolostone from Pozuelo de Aragón, Zaragoza, Spain (sample POZ02, table ST-1 in SI). The approximate size of the crystals is 6 µm. (b) Cretaceous massive dolostone from Alpedrete de la Sierra, Madrid, Spain (sample LB05, table ST-1 in SI)**.** The approximate size of the crystals is 56 µm.

X-ray powder diffraction of the samples confirmed that dolomite was the main rock-forming mineral (Figure 5a and Figure S1 in Supplementary Information, which also includes a zip file with raw diffractograms of all dolostone samples). Only in a few samples, calcite and more rarely quartz and gypsum were detected. SEM-EDX analyses performed on a selected number of thin sections allowed us to calculate dolomite chemical formulas (Figure 5b and Table ST-1 in Supplementary Information). Analysed dolomites have an average Mg/Ca ratio of 0.89 and most of them are almost stoichiometry (i.e., Mg/Ca = 1 ratio) with a slight excess of calcium. Only occasionally, iron and manganese were detected in amounts lower than 4% in the mineral formulas.

Table 1. Location in the map of Figure 2, number of samples analysed, geological epoch, geological environment, age, $I_{01.5}/I_{11.0}$ ratios, and $FWHM_{10.4}$ values of the dolomite samples studied.

Location in Figure 2	Number of samples	Geological epoch	Geological environment	Age (Myr)	I_{015}/I_{110}	$FWHM_{10.4}$
1	3	Holocene	Precipitation in caves	< 0.012	0	0.243 ± 0.073
2	1	Holocene	Precipitation in caves	< 0.012	0.418	0.405
3	1	Holocene	Continental deposits	< 0.012	0	0.231
4	2	Holocene	Continental deposits	< 0.012	0	0.246 ± 0.028
5	3	Pliocene	Maar Lake deposits	3.96 ± 1.39	0.509 ± 0.115	0.263 ± 0.038
6	1	Miocene	Continental basin	8.8 ± 1.5	0.564	0.212
7	4	Miocene	Continental basin	8.8 ± 1.5	0.453 ± 0.08	0.28 ± 0.021
8	1	Miocene	Continental basin	12.5 ± 1.4	0.42	0.261
9	3	Miocene	Continental basin	15.2 ± 1.5	0.542 ± 0.062	0.309 ± 0.057
10	3	Miocene	Continental basin	15.65 ± 1.87	0.58 ± 0.045	0.221 ± 0.005
11	1	Miocene	Continental basin	16.8 ± 3.2	0.451	0.278
12	2	Oligocene	Fluvial	41.5 ± 8.6	0.839 ± 0.188	0.225 ± 0.007
13	5	Upper Cretaceous	Marine	79.2 ± 7.5	0.709 ± 0.135	0.239 ± 0.061
14	11	Upper Cretaceous	Marine	87.9 ± 1.6	0.646 ± 0.149	0.225 ± 0.032
15	1	Upper Cretaceous	Marine	91.85 ± 2.05	0.516	0.215
16	4	Upper Cretaceous	Marine	94.8 ± 5	0.955 ± 0.137	0.2 ± 0.004
17	1	Upper Cretaceous	Marine	94.8 ± 5	0.902	0.206
18	1	Upper Cretaceous	Marine	94.8 ± 5	0.543	0.244
19	1	Upper Cretaceous	Marine	94.8 ± 5	0.574	0.212
20	1	Upper Cretaceous	Marine	97.2 ± 3.3	0.439	0.228
21	1	Lower Cretaceous	Marine	119 ± 6	0.584	0.323
22	2	Upper Jurassic	Marine	154.7 ± 2.6	0.67 ± 0.178	0.26 ± 0.001
23	5	Middle Jurassic	Marine	168.8 ± 5.3	0.715 ± 0.193	0.239 ± 0.012
24	6	Middle-Lower Jurassic	Marine	182.4 ± 18.9	0.512 ± 0.086	0.241 ± 0.021
25	2	Lower Jurassic	Marine	186.1 ± 4	0.646 ± 0.065	0.204 ± 0.011
26	2	Lower Jurassic	Marine	187.7 ± 13.6	0.883 ± 0.14	0.208 ± 0.014
27	1	Lower Jurassic	Marine	195.5 ± 3.5	0.744	0.212
28	19	Middle Triassic	Marine	242 ± 3	0.673 ± 0.128	0.214 ± 0.013
29	1	Middle Triassic	Marine	242 ± 3	0.706	0.23
30	3	Lower Devonian	Marine	413.5 ± 5.3	0.652 ± 0.078	0.219 ± 0.017
31	2	Upper Cambrian	Marine	516.5 ± 2.5	0.75 ± 0.306	0.212 ± 0.007
32	1	Precambrian	Marine	550 ± 5	0.66	0.221
33	5	Precambrian	Marine	620 ± 50	0.819 ± 0.104	0.208 ± 0.006
34	1	Precambrian	Marine	775 ± 225	0.863	0.228

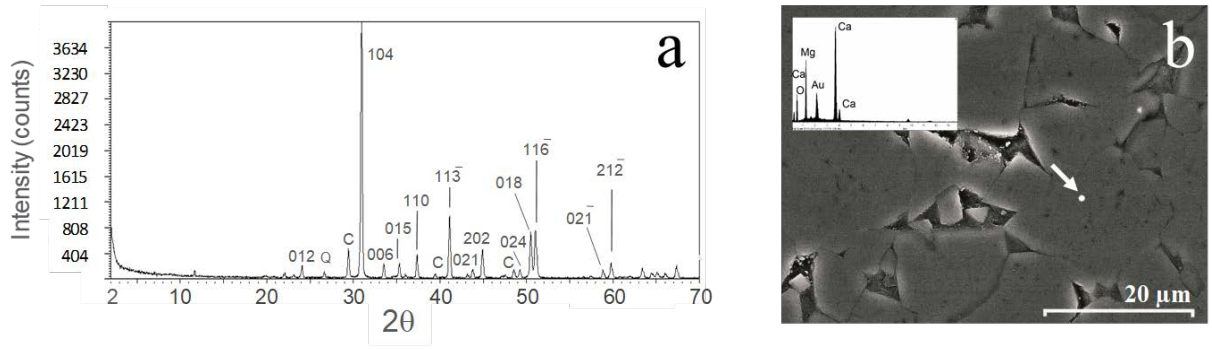

Figure 5. (a) X-ray powder diffractogram of a typical dolomite sample from the Lower Devonian (Barrios de Luna, León, Spain). Dolomite diffraction peaks have been indexed using the PDF file number 75-1710. Peaks corresponding to calcite and quartz impurities have been labelled as C and Q, respectively. Diffractograms of all dolostone samples are provided in a zip file in the Supplementary Information. (b) SEM image of thin section of the same dolomite sample. The inset shows an SEM-EDX analysis performed at the position indicated by the arrow. The dolomite formula calculated from this particular analysis is: $Mg_{0.86}Ca_{1.13}Fe_{0.01}(CO_3)_2$. All SEM-EDX analyses performed are listed in Table ST-1 in Supplementary Information.

A first analysis of the diffractograms provided values of the $I_{01.5}/I_{11.0}$ intensity ratios for all the dolomites collected (Table 1). Intensity ratios have been previously used by several authors to quantify the degree of cationic order of natural and synthetic dolomites (Graf and Goldschmidt, 1956; McKenzie, 1981; Hird, 1985; Böttcher et al., 1998; Luth, 2001; Hammouda et al., 2011; Kaczmarek and Sibley, 2011). This quantification is based on the fact that the relative intensity of the 01.5 diffraction peak in dolomite structure is directly related to the occupancy of magnesium and calcium atoms in alternate layers along the c-axis. Thus, when magnesium and calcium atoms are randomly distributed in such alternate layers, there is no cation order and, consequently, the 01.5 diffraction peak is absent in the diffractograms. Conversely, a perfect alternation of magnesium and calcium layers in the dolomite structure results in intensity maxima for the 01.5 peak. Thus, intermediate degrees of Mg-Ca order can be quantified by comparing the intensities of the 01.5 peak with the intensity of the 11.0 peak, the nearest diffraction peak with an intensity which is independent from cationic order (Figure 5a and Figure S1 in Supplementary Information).

Figure 6a shows average $I_{01.5}/I_{11.0}$ intensity ratios for dolomites of ages ranging from late Precambrian to late Holocene. Data points represented by black squares correspond to different geological formations studied in this work, whereas data points plotted as open circles were taken from the literature (see the caption of Figure 6a). The inclusion of data from previous works was done to confirm to some extent the consistency of our own data. Two error bars have been added to the data points. While vertical error bars display the standard deviation of measurements conducted on several samples from each geological formation, horizontal error bars indicate the uncertainty in the age of the dolomite formations described in the reviewed geological literature. As can be seen in the plot of Figure 6a, $I_{01.5}/I_{11.0}$ intensity ratios vary from zero (assigned to recent dolomites for which 01.5 peaks could not be resolved from diffractogram backgrounds) to around 0.8 for dolomites from late Cenozoic to late Precambrian (i.e., highly ordered dolomites). In this wide time interval, the maximum variation in the $I_{01.5}/I_{11.0}$ values is observed for dolomites formed in about the last 30 Myr.

The analysis of the diffractograms also provided values for the $FWHM_{10.4}$ (Table 1, column 7). The *FWHM* value of a diffraction peak can be considered as an indirect measure of the

crystallite size (or diffraction coherent domain) of polycrystalline samples, i.e., according to Scherrer equation the lower the *FWHM* value, the larger the coherent domain of the sample (Cullity and Stock, 2001). In the case of our dolomite samples, we have measured *FWHM* values on the 10.4 diffraction peak, i.e., the most characteristic and intense peak in dolomite diffractograms.

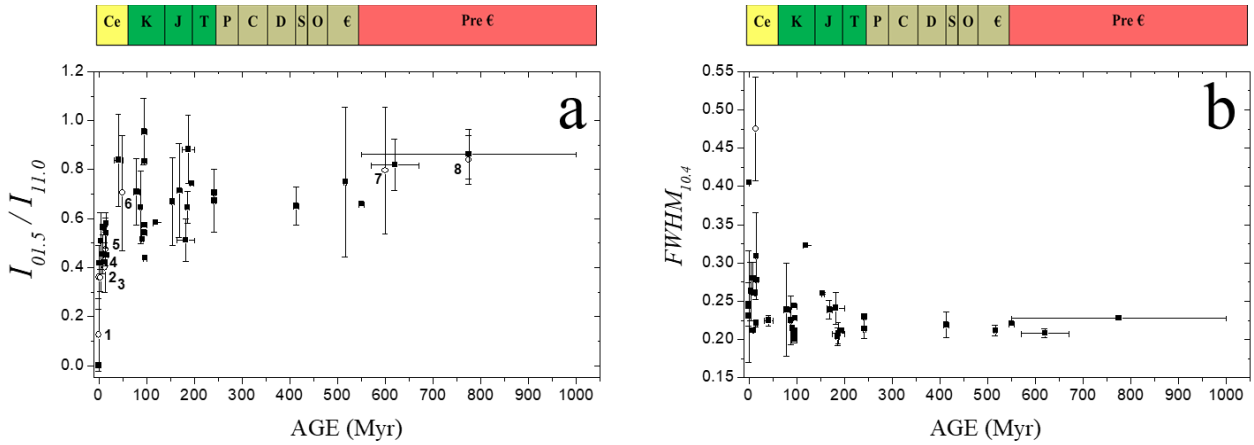

Figure 6. (a) $I_{01.5}/I_{11.0}$ intensity ratios versus dolomite age. Black squares: this work. Open circles with numbers: data from (1) dolomite speleothems of Castañar Cave (Alonso-Zarza and Martín-Pérez, 2008); (2) dolomites from shabkhas of Abu Dhabi (McKenzie, 1981); (3) lacustrine dolomites from La Roda (García del Cura et al., 2001); (4) lacustrine dolomites from Madrid basin (Leguey et al., 2010); (5) marine dolomites from Eratosthenes Seamount (Bottcher et al., 1998); (6) Zagros basin dolomites (Zohdi et al., 2014); (7) Porsanger diagenetic dolomites (Hird, 1985); (8) dolomites from Castañar de Ibor, Spain (Alonso-Zarza and Martín-Pérez, 2008). (b) $FWHM_{10.4}$ versus dolomite age. (black squares: this work; open circle: data from Böttcher et al., 1998). Upper colour bars: Ce: Cenozoic; K: Cretaceous; J: Jurassic; T: Triassic; P: Permian; C: Carboniferous; D: Devonian; S: Silurian; O: Ordovician; €: Cambrian; Pre €: Precambrian. Colour code: Cenozoic (yellow); Mesozoic (green); Palaeozoic (olive green); Precambrian (red).

Figure 6b shows average $FWHM_{10.4}$ values for dolomites formed in the last 775 Myr. As in the case of $I_{01.5}/I_{11.0}$ intensity ratios, vertical error bars display the standard deviation of $FWHM_{10.4}$ measurements, and horizontal error bars indicate ranges of age of the dolomite samples. These values vary from recent dolomites with $FWHM_{10.4}$ values above 0.25 (crystallite size below 37 nm) to older dolomites with $FWHM_{10.4}$ values around 0.22 (crystallite size around 42 nm). As in the case of the $I_{01.5}/I_{11.0}$ ratios, the maximum variation of $FWHM_{10.4}$ values is observed in about the last 30 Myr.

4 DISCUSSION

Data presented in the above section show clear variations in the cation order and $FWHM_{10.4}$ of dolomites formed in the last 775 Myr. These variations suggest a dolomite formation process extended for long periods of time during which cation order progressively increases. Thus, most of the dolomites formed in about the last 30 Myr have lower $I_{01.5}/I_{11.0}$ intensity ratios than older dolomites. In addition, over the last 30 Myr, $I_{01.5}/I_{11.0}$ values show an increasing trend with time, indicating that Mg-Ca ordering may occur for a long time after precipitation and sedimentation.

Even though systematic measurements of the variations of $I_{01.5}/I_{11.0}$ values with geological time have not been published to date, a few previous papers have reported interesting time-dependent variations of ordering in natural dolomites, which might support the idea that dolomitization can be a long-term process. Böttcher et al. (1998), for instance, measured relatively

low $I_{01.5}/I_{11.0}$ ratios for Pliocene and Miocene dolomites from Eratosthenes Seamount south of Cyprus (site 965 DSDP). These $I_{01.5}/I_{11.0}$ ratios increased with depth in the stratigraphic column from 0.39 to 0.56, reflecting that cationic order of the investigated dolomites also increases with their age. Similarly, Zohdi et al. (2014), who studied the older Eocene formation of Jahrum in Zagros Basin (Iran), measured average $I_{01.5}/I_{11.0}$ values of 0.71, i.e., significantly higher than those reported for the Pliocene and Miocene dolomites studied by Böttcher et al. (1998). Although Zohdi et al. (2014) did not report variations in the cationic order with time, their comparison of $^{87}Sr/^{86}Sr$ ratios of Jahrum dolostones and Cenozoic seawater showed that dolomitization occurred well after sedimentation and over an estimated time of approximately 15 Myr.

Although the number of crystallochemical investigations on modern dolomites is still scarce, published data show that the cation order of Holocene dolomites is typically lower than that of most Cenozoic dolomites. In this respect, McKenzie (1981), in her study on Holocene carbonate sediments from the shabkhas of Abu Dhabi, U.A.E, concluded that the dolomites found in such sediments were poorly ordered ($I_{01.5}/I_{11.0} = 0.36 \pm 0.13$) and resulted from an ageing process that lasted a few thousand years. After the publication of the paper by McKenzie, other authors have also reported that Holocene dolomites are generally poorly ordered (Mazzullo et al., 1987; Aqrawi, 1995; Alonso-Zarza and Martín-Pérez, 2008; Last et al., 2012; Turpin et al., 2012). These results are also consistent with a dolomitization process extended over long periods of time, which could not be completed within the short Holocene time.

The fact that a geological process, such as the formation of highly ordered dolomites, needs long periods of time to be completed is not infrequent. For instance, the formation of various geomaterials such as petroleum, natural gas and coal involves long-term reactions of ageing and maturing of the starting sedimentary material (i.e., phytoplankton, zooplankton and terrestrial plants). In the particular case of dolomite formation in nature, the ageing process mainly requires a mechanism which ensures the mobility and ordering of Mg and Ca within the dolomite structure. In this regard, $FWHM_{10.4}$ values of dolomites can provide relevant information about such a mechanism.

Li et al. (2015) reported that during the hydrothermal synthesis of dolomite, there is a positive correlation between $FWHM_{10.4}$ and the spacing $d_{10.4}$ of dolomite, and a negative correlation between such a spacing and the $I_{01.5}/I_{11.0}$ ratios. Thus, in the experiments conducted by Li et al. (2015), the progressive Mg-Ca ordering of dolomite positively correlates with a decrease in the values of $FWHM_{10.4}$.

A similar correlation between degree of cation order and $FWHM_{10.4}$ has been detected during the formation of the dolomite-analogue mineral norsethite, $BaMg(CO_3)_2$ (Pimentel and Pina, 2014). In a series of experiments conducted at ambient conditions, Pimentel and Pina (2014) observed that, during the first stages of norsethite crystallisation from an amorphous precursor, Ba-Mg ordering (quantified through $I_{01.5}/I_{00.6}$ and $I_{10.1}/I_{01.2}$ ratios) improved while $FWHM_{10.4}$ of the evolving precipitate decreased (i.e., norsethite crystallite size tended to increase).

As in the case of hydrothermal dolomites (Li et al., 2015) and the dolomite analogue norsethite (Pimentel and Pina, 2014), cation ordering and $FWHM_{10.4}$ of the natural dolomites studied in the present work seem to be related. In Figure 7, $FWHM_{10.4}$ versus $I_{01.5}/I_{11.0}$ ratios have been plotted. As can be seen in this figure, an increase in $I_{01.5}/I_{11.0}$ ratios between ~0.4 and ~0.6 is mostly accompanied by a decrease in $FWHM_{10.4}$ values from about 0.40 to about 0.20, i.e. an increase in the crystallite size of dolomites from 23 nm to 45 nm, calculated with the Scherrer equation (Scherrer, 1918; Cullity and Stock, 2001). For $I_{01.5}/I_{11.0}$ ratios higher than 0.6, $FWHM_{10.4}$ remains at an almost constant value of about 0.22 (i.e. a crystallite size of 42 nm, approximately).

Only very recent dolomites for which $I_{01.5}/I_{11.0}$ ratios were assumed to be zero, deviate from this general trend, suggesting that their degree of order has been underestimated.

The decrease of $FWHM_{10.4}$ values and the corresponding increase in the size of the coherent diffraction domain is the result of a ripening process that reduces the number of grain boundaries (Scherrer, 1918; Cullity and Stock, 2001). At ambient conditions and in systems where aqueous solutions are present, this usually occurs by dissolution-(re)crystallisation. In the case of dolomite formation, dissolution of small mineral grains in favour of the growth of larger crystals accompanied by an increase of cation order in the dolomite structure might be promoted by physicochemical fluctuations at a local scale within the initial sediments (Deelman, 1999). These fluctuations can consist of cyclic variations in pH, temperature, salinity and/or composition ratios. Therefore, if we consider that the formation conditions of the natural dolomites studied in our work preclude effective solid state ionic diffusion, data plotted in Figure 7 suggest that a dissolution-(re)crystallisation process operating over large geological periods lead to a progressive increase in the cation order of dolomites. The operation of such a dissolution-(re)crystallisation process during the formation of dolomites is further supported by the fact that the presence of well-preserved fossils is much less frequent in dolostones than in limestones (Deelman, 2011 and references therein). This indicates that shells and other calcium carbonate-based bioconstructions were partially or totally erased as a consequence of the (re)crystallisation of precursor carbonates (e.g., Mg-calcite, aragonite and poorly ordered dolomites).

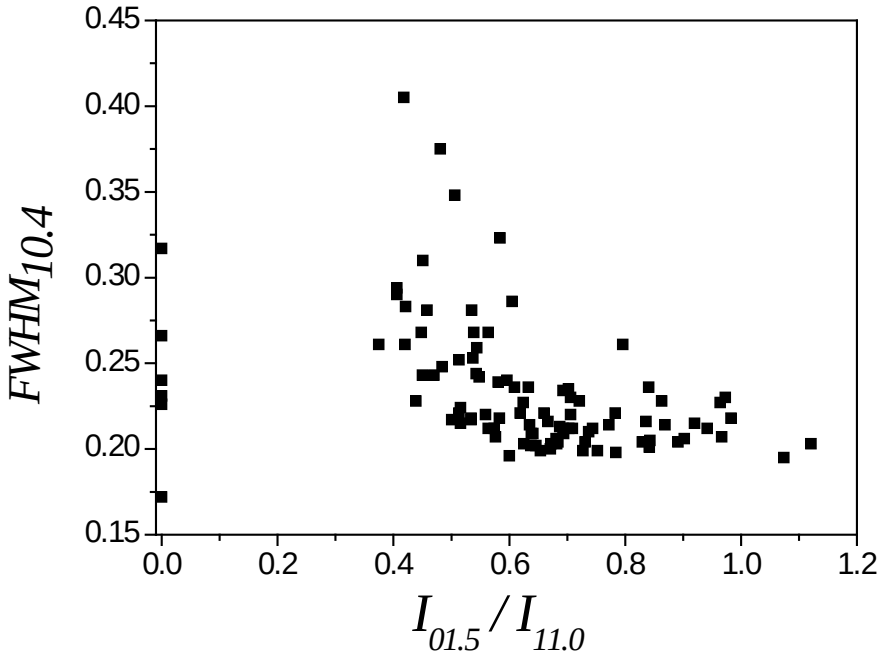

Figure 7. $FWHM_{10.4}$ versus $I_{01.5}/I_{11.0}$ for all samples studied in this work.

Nevertheless, the efficiency of dissolution-(re)crystallisation as a mechanism of cation ordering in dolomites is affected by a number of factors. Probably, one of the most relevant is the Mg/Ca ratio of the precursor carbonates of dolomites. It is apparent that deviations from dolomite stoichiometry (Mg/Ca = 1) preclude complete cation order. This is due to the fact that magnesium or calcium excess in dolomite formulas makes an alternation of pure Mg and Ca layers along the dolomite structure *c* axis impossible. Figure 8 shows $I_{01.5}/I_{11.0}$ ratios versus Mg/Ca ratios of a

number of dolomites studied in this work. Interestingly, no correlation between $I_{01.5}/I_{11.0}$ order and Mg/Ca ratios is observed. This indicates that deviations of dolomite Mg/Ca ratios from unity have a relatively minor effect on the cation order. Thus, for a given Mg/Ca ratio, different $I_{01.5}/I_{11.0}$ ratios for dolomites of various ages have been measured, which reflects a progressive ordering process.

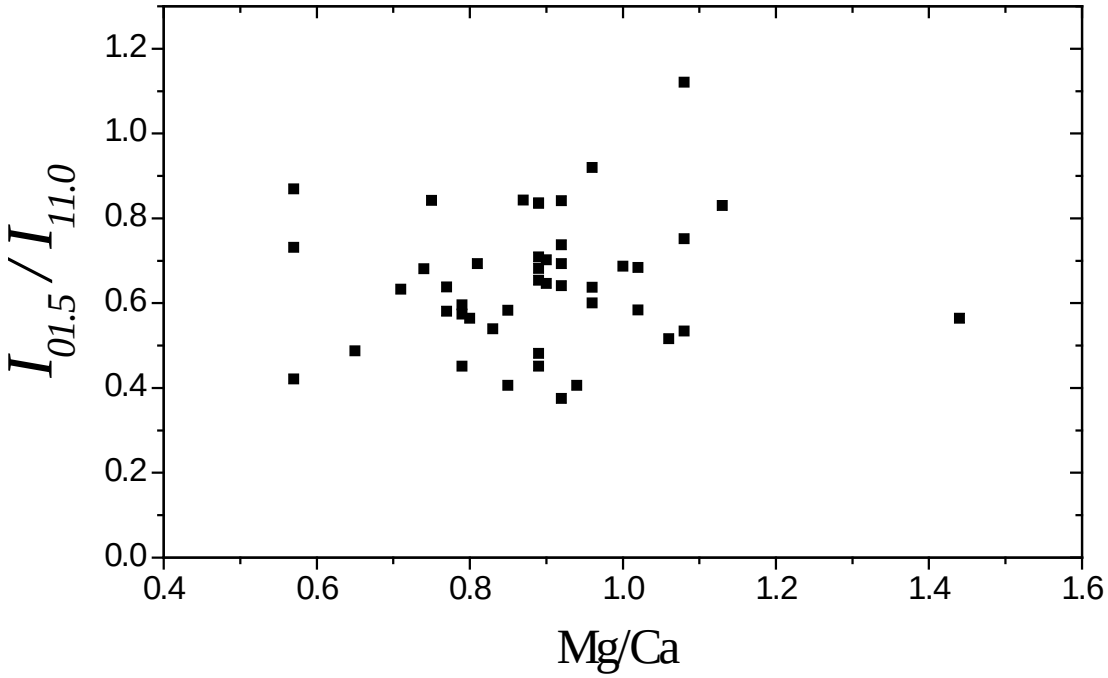

Figure 8. Dolomite $I_{01.5}/I_{11.0}$ versus Mg/Ca ratios. Note the scattering of the $I_{01.5}/I_{11.0}$ values for a given Mg/Ca ratio.

This Mg-Ca ordering process requires a wet environment that guarantees a more or less continuous dissolution and (re)crystallisation of initial carbonate mineral grains with adequate Mg/Ca ratios. In such a wet environment, both fluctuations in groundwater levels related to local hydrological cycles and long-term variations in the composition and transport of geological fluids can affect the kinetics of cation ordering. Furthermore, the existence of fluxes and refluxes of fluids (i.e., more or less modified seawater, diapir-derived fluids, etc.) through the carbonate sediments can also play a fundamental role in dolomitization (Warrren, 2000 and references therein; Haldar and Tisljar, 2014; Nokhbatolfoghahaei et al., 2019).

Our data indicate that cation ordering in natural dolomites takes place over long periods of time. However, the precise knowledge of the time-scale within dolomitization and dolomite cation ordering occurs in nature is still an open question. In this regard, some experimental works have provided valuable information. In 1989, Usdowski reported the results of a series of long-term experiments addressed to crystallise dolomite by reacting aragonite powders with magnesium and calcium chlorides at 60 ºC (Usdowski, 1989, 1994). In his papers, Usdowski claimed to have observed the formation of dolomite after 7 years of reaction. On the basis of this result, Usdowski (1989) hypothesized that dolomite formation is a process which can require hundreds to thousands of years. In contrast, after conducting even more longer term experiments at 25ºC, Land (1998) concluded that dolomite did not form after 32 years from a very highly supersaturation with respect to this mineral. Differently, Lieberman (1967) and Deelman (1999) claimed to have synthesised dolomite after a few weeks by inducing dissolution-precipitation cycles on slurries containing

calcium and magnesium carbonates. Unfortunately, these researchers did not provide diffractograms with clearly recognisable ordering peaks at different reaction times. Therefore, the kinetics of the dolomite cationic ordering process cannot be quantified.

Very recently, Kell-Duivestein et al. (2019) reported the synthesis of dolomite by reacting calcite and aragonite with a $MgCl_2$ and $NaHCO_3$ solution over one year and at temperatures of 150 °C, 180 °C and 220 °C. By extrapolating dolomitization rates obtaining in their synthesis experiments, Kell-Duivestein et al. (2019) concluded that, near room temperature, millions of years can be required to form fully ordered dolomite in nature. This conclusion is very relevant since provides a temporal framework for the formation of dolomite in sedimentary and postsedimentary environments. Remarkably, a timescale of millions of years for dolomite formation is consistent with the results presented in this paper.

5 CONCLUSIONS AND OUTLOOK

By analysing X-ray powder diffractograms, we have quantified the degree of cation order and $FWHM_{10.4}$ of more than 100 sedimentary Iberian dolomites of ages ranging from Neoproterozoic to Holocene. Diffractograms showed that dolomites older than about 30 Myr have typically higher $I_{01.5}/I_{11.0}$ ratios (i.e., higher cationic order) and lower $FWHM_{10.4}$ values (i.e., larger crystallite sizes) than dolomites formed in more recent geological times (i.e., late Cenozoic and Holocene). Moreover, within late Cenozoic and Holocene, $I_{01.5}/I_{11.0}$ values seem to progressively increase with time, indicating that Mg-Ca ordering may occur over long periods of time. Such an increase in cation order is consistent with data previously published on a reduced number of samples of natural dolomites from various geological formations.

Interestingly, $I_{01.5}/I_{11.0}$ and $FWHM_{10.4}$ seems to be related and, usually, highly ordered dolomites also show low $FWHM_{10.4}$ values. If we assume that a progressive a decrease in $FWHM_{10.4}$ (i.e. an increase in crystallite size) reveals mineral ripening, our data suggest that cation ordering in natural dolomites can occur by a dissolution-(re)crystallisation process extended over time scales, which largely exceed those of any human experiment conducted under similar conditions, i.e., thousands to millions of years.

However, even though dolomite formation seems to be a longstanding process, a detailed analysis of the factors which determines the kinetics of Mg-Ca ordering in dolomites is beyond the scope of this paper. Thus, in this work, we did not quantify stoichiometric and impurity effects on cation ordering (i.e., the effect of Ca or Mg excess on the $I_{01.5}/I_{11.0}$ ratios and the incorporation of Fe and Mn into dolomite structure). We did not take into account either geochemical factors (e.g., Mg and Ca concentrations of aqueous solutions, circulation of fluids, wet and dry cycles during dolomite formation, temperature and pH fluctuations, etc.), which can promote or retard cation ordering in dolomites by a dissolution-(re)crystallisation mechanism. Obviously, future research should consider these and other factors to better define the time variability of $I_{01.5}/I_{11.0}$ ratios and $FWHM_{10.4}$ values of dolomites in the geological record. This information could be used to develop rock dating methods based on the cation order and/or crystallite size of natural dolomites. However, to significantly improve our knowledge of the crystallochemical features of natural dolomites, further mineralogical and structural analyses (e.g., using the Rietveld method and/or new approaches to quantify cation order and Mg/Ca ratios (e.g., Shen et al., 2014; Fang and Xu, 2019)) of a larger number of samples from geological formations all over the world are clearly needed.

ACKNOWLEDGMENTS

The authors thank Marcos Endrina, Claudia Finotelli, Óscar García Monasterio and Yuliya Zvir for their assistance with sample collection and preparation. We also thank Ana Alonso-Zarza, Esther Sanz and Jaime Cuevas for providing three dolomite samples. This work was partially supported by the Spanish Government (Project CGL2017-85118-P). SEM images and EDX analyses were obtained at the ICTS Centro Nacional de Microscopía Electrónica, (UCM) Madrid.

SUPPLEMENTARY DATA

In the supplementary data files can be found:

- Table ST-1: More detailed version of Table 1 with coordinates of the locations where dolomite samples were collected and chemical formulas of dolomites analysed by SEM-EDX.
- Figure S-1. Diffractograms of three dolomites with different degree of cation order.
- Diffractograms: Raw files of diffractograms of all samples classified by geological epochs are provided in a zip file.

REFERENCES

Alonso-Zarza, A. M., Martín-Pérez, R. (2008) Dolomite in caves: Recent dolomite formation in oxic, non-sulfate environments. Castañar Cave, Spain. *Sedimentary Geology* **205**, 160 – 164.

Aqrawi, A.A.M. (1995) Brackish-water and evaporitic Ca-Mg carbonates in the Holocene lacustrine/deltaic deposits of Southern Mesopotamia. *Journal of the Geological Society*, London **152**, 259-268

Böttcher, M. E., Mart, Y., Brumsack, H.-J. (1998) 35. Data report: geochemistry of Pliocene and Miocene carbonates from the Eratosthenes seamount (site 965). *Proceedings of the Ocean Drilling Program, Scientific Results* **160**, 447 – 451.

Burns, S. J., Mckenzie J. A, Vasconcelos C. (2000) Dolomite formation and biogeochemical cycles in the Phanerozoic. *Sedimentology* **47** (1), 49-61.

Cullity, B.D., Stock, S.R. (2001) *Elements of X-Ray Diffraction, 3rd Ed.* Prentice-Hall Inc.

De Dolomieu, D.G. (1791) Sur un de pierres trés-peu effervescentes avec les acides of phosphorescentes par la collision. *Journal de Physique* **39**, 3–10. (in French).

Deelman, J.C. (1999) Low-temperature nucleation of magnesite and dolomite. *Neues Jahrbuch für Mineralogie, Monatshefte* **7**, 289 – 302.

Deelman, J.C. (2011) Low-Temperature formation of dolomite and magnesite: version 2.3, 512 p.

Fang, Y., Xu, H. (2019) A New Approach To Quantify the Ordering State of Protodolomite Using XRD, TEM, and Z-Contrast Imaging. *Journal of Sedimentary Research* **89**, 537 - 551.

Gaines, A.M. (1977) Protodolomite redefined. *Journal of Sedimentary Petrology* **47**, 543 – 546.

García del Cura, M. A., Calvo, J. P., Ordoñez, S., Jones, B. F., Cañaveras, J. C. (2001) Petrographic and geochemical evidence for the formation of primary, bacterially induced lacustrine dolomite: La Roda 'white earth' (Pliocene, central Spain). *Sedimentology* **48**, 897 – 915.

Given, R.K. and Wilkinson, B.H. (1987) Dolomite abundance and stratigraphic age: constraints on rates and mechanisms of Phanerozoic dolostone formation. *Journal of Sedimentary Research* **57** (6), 1068-1078.

Graf, D. L., Goldsmith, J. R. (1956) Some hydrothermal synthesis of dolomite and protodolomite. *Journal of Geology* **64**, 173 – 187.

Gregg, J. M., Bish, D. L., Kaczmarek, S. E., Machel, H. G. (2015) Mineralogy, nucleation and growth of dolomite in the laboratory and sedimentary environment: A review. *Sedimentology* **62**, 1749 – 1769.

Haldar, S. K., Tisljar, J. (2014) Sedimentary rocks. In: *Introduction to Mineralogy and Petrology* (Haldar and Tisljar, Eds.), p 121 – 212. Elsevier.

Hammouda, T., Andrault, D., Koga, K., Katsura, T., Martin, A. M. (2011) Ordering in double carbonates and implications for processes at subduction zones. *Contributions to Mineralogy and Petrology* **161**, 439 – 450

Hird, K. (1985) Petrography and geochemistry of some Carboniferous and Precambrian dolomites. Durham theses, Durham University. Available at Durham E-Theses Online: http://etheses.dur.ac.uk/1674/

Kell-Duivestein, I.J., Baldermann, A., Mavromatis, V., Dietzel, M. (2019) Controls of temperature,alkalinity and calcium carbonate reactant on the evolution of dolomite and magnesite stoichiometry and dolomite cation ordering degree-An experimental approach. Chemical Geology **529**, 119292. doi.org/10.1016/j.chemgeo.2019.119292.

Kaczmarek, S. E., Sibley, D. F. (2011) On the evolution of dolomite stoichiometry and cation order during high-temperature synthesis experiments: An alternative model for the geochemical evolution of natural dolomites. *Sedimentary Geology* **240**, 30 – 40.

Land, L. S. (1998) Failure to precipitate dolomite at 25 ºC from dilute solution despite 1000-fold oversaturation after 32 years. *Aquatic Geochemistry* **4**, 361 – 368.

Last, F.M., Last, W.M., Halden, N.M. (2012) Modern and late Holocene dolomite formation_ Manito Lake, Saskatchewan, Canada. *Sedimentary Geology* **281**, 222-237

Li, W., Beard, B.L., Li, C., Xu, H. and Johnson, C.M. (2015) Experimental calibration 812 of Mg isotope fractionation between dolomite and aqueous solution and its geological implications. *Geochimica et Cosmochimica Acta* **157**, 164-181.

Liebermann, O. (1967) Synthesis of dolomite. *Nature* **213**, 241 – 245.

Lu, Y., Sun, X., Xu, H., Konishi, H., Lin, Z., Xu, L., Chen, T., Hao, X., Lu, H., Peckmann, J. (2018) Formation of dolomite catalyzed by sulfate-driven anaerobic oxidation of methane: Mineralogical and geochemical evidence from the northern South China Sea. *American Mineralogist* **103**(5), 720 – 734. doi: https://doi.org/10.2138/am-2018-6226

Luth, R. W. (2001) Experimental determination of the reaction aragonite + magnesite = dolomite at 5 to 9 GPa. *Contributions to Mineralogy and Petrology* **141**, 222 – 232.

Martin, J. D. (2008) A software package for Powder X-Ray Diffraction analysis. ISBN: 84-609-1497-6

Mazzullo, S.J., Reid, A.M., Gregg, J.M. (1987) Dolomitization of Holocene Mg-calcite supratidal deposits, Ambergris Cay; Belize. *Geological Society of America Bulletin* **98**, 224-231.

McKenzie, J. **(**1981) Holocene dolomitization of calcium carbonate sediments from the coastal sabkhas of Abu Dhabi, U.A.E.; A stable isotope study. *Journal of Geology* **89**, 185-98.

Nokhbatolfoghahaei, A., Nezafati, N., Ghorbani, M., Abdolabadi, B. E. (2019) Evidence for origin and alteration in the dolomites of salt diapirs, Larestan, Southern Iran. *Carbonates Evaporites* **34**, 389 - 403. https://doi.org/10.1007/s13146-017-0399-5.

Pimentel C. and Pina C. M. (2014) The formation of the dolomite analogue norsethite: reaction pathway and cation ordering. *Geochimica et Cosmochmica Acta* **142**, 217–233.

Pimentel, C. and Pina, C.M. (2016) Reaction pathways towards the formation of dolomite-analogues at ambient conditions. *Geochimica et Cosmochimica Acta* **178** , 259-267.

Riding, R. and Liang, L. (2005) Seawater chemistry control of marine limestone accumulation over the past 550 million years. *Revista Española de Micropaleontología* **37**(1), 1 -11.

Scherrer, P. (1918) Estimation of the size and internal structure of colloidal particles by means of Röntgen rays. *Göttinger Nachrichten Math. Phys*. **2**, 98–100.

Schultz-Güttler, R. (1986) The influence of disordered, non-equilibrium dolomites on the Mg-solubility in calcite in the system $CaCO_3 – MgCO_3$. *Contributions to Mineralogy and Petrology* **93**, 395 – 398.

Shen, Z., Konishi, H., Szlufarska, I., Brown, P. E., Xu, H. (2014) Z-contrast imaging and ab initio study on "d" superstructure in sedimentary dolomite. *American mineralogist* **99**, 1413-1419.Turpin, M., Nader, F.H., Kohler, E. (2012) Empirical Calibration for Dolomite Stoichiometry Calculation: Application on Triassic Muschelkalk-Lettenkohle Carbonates (French Jura). *Oil and Gas Science and Technology, IFPE Energies Nouvelles* **67**, 77-95.

Usdowski, E. (1989) Synthesis of dolomite and magnesite at 60 ºC in the system $Ca^{2+}Mg^{2+}$-CO_3^{2-}-Cl_2^{2-}-H_2O. *Naturwissenschafen* **76**, 374 – 375.

Usdowski, E. (1994) Synthesis of dolomite and geochemical implications. In: Dolomites: A volume in honour of Dolomieu (B. Purser, M. Tucker, D. Zenger, Eds), Wiley, 345 - 360.

Warren, J. (2000) Dolomite: occurrence, evolution and economically important associations. *Earth-Science Reviews* **52**, 1 – 81.

Zohdi, A., Moallemi, S.A., Moussavi-Harami, R., Mahboubi, A., Richter, D.K., Geske, A., Nickandish, A.A., Immenhauser, A. (2014) Shallow burial dolomitization of an Eocene carbonate platform, southeast Zagros Basin, Iran. *GeoArabia* **19 (4)**, 17-54.